Discrete Laplace Operator on Meshed Surfaces

[Extended Abstract]

Mikhail Belkin
Dept. of Comp. Sci. & Eng.
The Ohio State University
Columbus OH 43210
mbelkin@cse.ohio-state.edu

Jian Sun
Dept. of Comp. Sci.
Stanford University
Palo Alto CA 94305
sunjian@stanford.edu

Yusu Wang
Dept. of Comp. Sci. & Eng.
The Ohio State University
Columbus OH 43210
yusu@cse.ohio-state.edu

ABSTRACT

In recent years a considerable amount of work in graphics and geometric optimization used tools based on the Laplace-Beltrami operator on a surface. The applications of the Laplacian include mesh editing, surface smoothing, and shape interpolations among others. However, it has been shown [13, 24, 26] that the popular cotangent approximation schemes do not provide convergent point-wise (or even $\mathcal{L}_2$) estimates, while many applications rely on point-wise estimation. Existence of such schemes has been an open question [13].

In this paper we propose the first algorithm for approximating the Laplace operator of a surface from a mesh with point-wise convergence guarantees applicable to arbitrary meshed surfaces. We show that for a sufficiently fine mesh over an arbitrary surface, our mesh Laplacian is close to the Laplace-Beltrami operator on the surface at every point of the surface.

Moreover, the proposed algorithm is simple and easily implementable. Experimental evidence shows that our algorithm exhibits convergence empirically and compares favorably with cotangent-based methods in providing accurate approximation of the Laplace operator for various meshes.

Categories and Subject Descriptors

G.2 [**Mathematics of Computing**]: Discrete mathematics

General Terms

Algorithms, Theory, Experimentation

Keywords

Laplace-Beltrami operator, Surface mesh, Approximation algorithm

1. INTRODUCTION

A broad range of topics in geometric modeling and computer graphics is concerned with processing two-dimensional surfaces in a three-dimensional space. These surfaces are typically represented by a mesh, which is given by the coordinates of its vertices and the connectivity information. Thus, manipulating, deforming and analyzing meshed surfaces is a crucial area within these subjects, with the usual implicit assumption that processing of a mesh corresponds to analogous processing of the underlying surface.

In recent years a class of methods based on discrete differential geometry of surfaces [1] and the discrete Laplace operator has been used for various tasks of geometric processing. For example, the state-of-the-art report on Laplacian Mesh Processing [21] discusses surface reconstruction, mesh editing, shape representation and shape interpolation among other applications of Laplacian-based mesh processing methods. Such applications of the Laplacian can be found in [3, 10, 12, 22, 23, 27] among others.

The Laplace-Beltrami operator (manifold Laplacian) is a fundamental geometric object associated to a Riemannian manifold and has many desirable properties. The Laplacian can be used as a smoothness penalty to choose functions varying smoothly along the manifold [23] or to smooth the surface itself via the *mean curvature flow* [10], which is determined by applying the Laplace operator to coordinate functions x, y, z considered as functions on the surface. Moreover, eigenfunctions of the Laplacian form a natural basis for square integrable functions on the manifold analogous to Fourier harmonics for functions on a circle (i.e. periodic functions). Therefore, computing eigenfunctions of a Laplacian allows one to construct a basis reflecting the geometry of the surface [12]. Finally, the Laplace operator is intimately related to diffusion and the heat equation on the surface, and is connected to a large body of classical mathematics, relating geometry of a manifold to the properties of the heat flow (see, e.g., [20]).

Several discretizations of the Laplacian for an arbitrary mesh have been proposed [9, 10, 14, 19, 23, 25]. Most of the proposed methods are variants of the *cotangent scheme* [19], which is a form of the finite element method, applied to the Laplace operator on a surface. Suppose we have a surface with a fine mesh. We expect that the discretization computed from such a mesh would be an accurate representation of the underlying surface Laplacian. However, a detailed theoretical analysis of existing discretizations in [25, 26] shows that while point-wise convergence can be established for special classes of meshes, such as certain meshes with valence 6, or for linear functions over a sphere in $\mathbb{R}^3$, none of these methods can be expected to converge for surface meshes in general, a finding, which is borne out by experimental results in Section 5 and [26]. A notable recent work is [13, 24], where the authors analyze convergence of various geometric invariants, including Laplace-Beltrami operators. They apply their analysis to the popular cotangent scheme showing *weak convergence* (in the distribution sense) for the solution of the Dirichlet's problem, assuming the aspect ratio of mesh elements is bounded. The authors also

demonstrate that under the cotangent scheme, convergence in $\mathcal{L}_2$ (which is weaker than point-wise convergence) does not generally hold.

The results presented in our paper provide the first discretization scheme that guarantees convergence at each point (i.e, $\mathcal{L}_\infty$ and thus also $\mathcal{L}_2$ convergence). Moreover, by using some recent results [2], it can be shown that convergence of eigenfunctions also follows.

We note that while $\mathcal{L}_\infty$ convergence is required in many applications, where various quantities, e.g., mean curvature, need to be estimated at each node of the mesh, the construction of such a scheme is not trivial. For example, in [13] (Section 4.3.2) the authors conjecture that no such discretizations may exist.

We summarize the contributions of the paper as follows:

1. We propose a simple method for approximating integrals over a surface using a mesh and analyze the quality of the resulting approximation in terms of the parameters of the surface and the mesh.

2. Combining the integral approximation results with the idea of approximating the heat flow on a mesh, we present and analyze the first algorithm for approximating Laplace-Beltrami operator on a surface with point-wise convergence guarantees for arbitrary meshes.

3. The resulting algorithm is simple and straightforward to implement. We provide experimental results showing that it outperforms the cotangent scheme in approximation quality and robustness to noise.

We note that the algorithm for computing the surface Laplacian is related to the set of algorithms for computing Laplacian of point clouds in data analysis and machine learning [7, 8] by using the heat equation. We observe that in machine learning, the samples are usually believed to be drawn *independently* from a probability distribution and the convergence occurs in probability. On the other hand, in surface modeling, the nodes of a mesh are typically not sampled independently from a probability distribution but are generated by some deterministic process, e.g. scanning. Hence in the case of mesh Laplacian, approximation guarantees need to be made for *all* sufficiently fine meshes, and probabilistic techniques based on the law of large numbers (usually used in the case of randomly sampled point clouds) cannot be applied.

2. ALGORITHM AND OVERVIEW OF THE RESULTS

2.1 Mesh Laplacian Algorithm

We start by describing our algorithm for computing the Laplace operator on a meshed surface. Let K be a mesh in $\mathbb{R}^3$. We denote the set of vertices of the mesh K by V. Given a face, a mesh, or a surface X, let $\mathrm{Area}(X)$ denote the area of X. For a face $t \in K$, the number of vertices in t is denoted by $\#t$, and $V(t)$ is the set of vertices of t.

Our algorithm takes a function $f : V \to \mathbb{R}$ as **input** and produces another function $\mathrm{L}_K^h f : V \to \mathbb{R}$ as **output**. L_K^h, the **mesh Laplace operator**, is computed, for any $w \in V$, as follows:

$$\mathrm{L}_K^h f(w) = \frac{1}{4\pi h^2} \sum_{t \in K} \frac{\mathrm{Area}(t)}{\#t} \sum_{p \in V(t)} e^{-\frac{\|p-w\|^2}{4h}} (f(p) - f(w))$$
(1)

The **parameter** h is a positive quantity, which intuitively corresponds to the size of the neighborhood considered at each point. In many applications and for the theoretical analysis in this paper h is taken to be independent of the point w. However, in general, h can be taken to be a function of w, which will allow the algorithm to adapt to the local mesh size.

The theoretical results in this paper show that when K is a sufficiently fine mesh of a smooth underlying surface S, L_K^h is close to the surface Laplacian Δ_S (the formal definition will be introduced shortly). Indeed, our preliminary experimental results demonstrate the converging behavior of this operator, and show that our algorithm outperforms currently available discrete Laplace operators in the approximation quality.

In the remainder of this section, after introducing necessary notations, we give an outline of the theoretical results, which also explains the derivation of this algorithm.

2.2 Objects and Notations

Surface Laplace operator Δ_S. In this paper, we consider a smooth compact 2-manifold S without boundary isometrically embedded in some Euclidean space $\mathbb{R}^3$ with geometry induced by the embedding. (Note that any such surface is necessarily orientable.) The corresponding *volume form*, denoted by ν, determines the area of a surface element. We assume that S is connected — surfaces with multiple components can be handled by applying our results in a component-wise manner.

Given a twice continuously differentiable function $f \in C^2(S)$, let $\nabla_S f$ denote the gradient vector field of f on S. The Laplace-Beltrami operator Δ_S of f is defined as the divergence of the gradient; that is, $\Delta_S f = \mathrm{div}(\nabla_S f)$. For example, if S is a domain in $\mathbb{R}^2$, then the Laplacian has the familiar form $\Delta_{\mathbb{R}^2} f = \frac{\partial^2 f}{\partial x^2} + \frac{\partial^2 f}{\partial y^2}$.

Functional Laplacian F_S^h. To connect the mesh Laplace operator L_K^h, as defined in Eqn (1), with the surface Laplacian Δ_S, we need an intermediate object, called the *functional Laplace operator* F_S^h. Given a point $w \in S$ and a function $f : S \to \mathbb{R}$, it is defined as follows:

$$\mathrm{F}_S^h f(w) = \frac{1}{4\pi h^2} \int_{x \in S} e^{-\frac{\|x-w\|^2}{4h}} (f(x) - f(w)) \, d\nu(x). \quad (2)$$

Definition of (ε, η)-approximation. We also need a quantitative measure of how well a mesh approximates the underlying surface. Let the *medial axis M of S* be the closure of the set of points in $\mathbb{R}^3$ that have at least two closest points in S. For any $w \in S$, the *local feature size at w*, denoted by $\mathrm{lfs}(w)$, is the distance from w to the medial axis M. The *reach* (also known as the condition number) $\rho(S)$ of S is the infimum of the local feature size at any point in S. At each point $p \in S$, n_p denotes the *unit* outward normal of S at p and for each face $t \in K$, n_t is the unit outward normal of the plane passing through t.

In the paper, we assume that the vertices of the mesh K lie on the surface S. Let ρ be the reach of S. We say that K is an (ε, η)-*approximation* of S, if the following conditions hold:

1. For a face $t \in K$, its diameter (maximum distance between any two points on t) is at most $\varepsilon\rho$.

2. For a face $t \in K$ and a vertex $p \in t$, the angle between vectors n_t and n_p, $\angle(n_t, n_p)$, is at most η.

Intuitively, the first condition ensures that the mesh is sufficiently fine. On the other hand, a very fine mesh can still provide a poor approximation to the underlying surface, as, for example, is seen in the Schwarz lantern. Thus the second condition is also necessary to ensure the closeness between K and S.

In many cases, we work with triangular meshes. Note the approximation conditions do not require that the triangles in K are well-shaped, for instance having small aspect ratio. However the second condition can be implied if we assume that there exists at least one angle whose sin is bounded from below for each triangle [16], which is a much weaker condition than small aspect ratio. Note that many surface reconstruction algorithms (see [11]) produce meshes that satisfy these conditions.

Our technical results use the analysis of the map $\phi : K \to S$ defined as follows: For any $p \in K$, $\phi(p)$ is defined as the closest point to p on the surface S. ϕ is well-defined when K avoids the medial axis of S, which will be the case in our setting. The map ϕ connects the mesh K with the surface S, and is widely used in analyzing surface reconstruction algorithms [4, 11], as well as in approximating various quantities for smooth surfaces [13, 16].

2.3 Overview of the Main Results

Our main result is Theorem 2.1. Intuitively, as the mesh approximating the surface S becomes denser, the mesh Laplace operator on K converges to the Laplace-Beltrami operator of S.

Theorem 2.1 *Let the mesh $K_{\varepsilon,\eta}$ be an (ε, η)-approximation of S. Put $h(\varepsilon, \eta) = \varepsilon^{\frac{1}{2.5+\alpha}} + \eta^{\frac{1}{1+\alpha}}$ for an arbitrary fixed positive number $\alpha > 0$. Then for any $f \in C^2(S)$*

$$\lim_{\varepsilon,\eta \to 0} \sup_{K_{\varepsilon,\eta}} \left\| \mathrm{L}_{K_{\varepsilon,\eta}}^{h(\varepsilon,\eta)} f - \Delta_S f \right\|_{\infty} = 0 \quad (3)$$

where the supremum is taken over all (ε, η) approximations of S.

It is important to note that for a triangular mesh, we can obtain the following corollary which says that the convergence result still holds if we replace the second condition in (ε, η)-approximation by requiring the triangles to be well-conditioned, which is an easily verifiable condition.

Corollary 2.2 *Let K_ε be a triangular mesh with all the vertices on S and the diameter of each triangle less than $\varepsilon\rho$. In addition, let $s(t) = \max_{p \in V(t)} \sin(\theta_p)$ where θ_p is the angle of the triangle t at vertex p, and assume that $s(K) = \min_{t \in K} s(t)$ is bound from below by some constant. Put $h(\varepsilon) = \varepsilon^{\frac{1}{2.5+\alpha}}$ for an arbitrary fixed positive number $\alpha > 0$. Then for any $f \in C^2(S)$*

$$\lim_{\varepsilon \to 0} \sup_{K_\varepsilon} \left\| \mathrm{L}_{K_\varepsilon}^{h(\varepsilon)} f - \Delta_S f \right\|_{\infty} = 0 \quad (4)$$

where the supremum is taken over all such triangular meshes.

Corollary 2.2 follows immediately from Theorem 2.1 and Corollary 1 in [16] which says $\sin \angle(n_t, n_p) < (\frac{4}{s(K)} + 2)\varepsilon$ for any triangle $t \in K$ and any $p \in V(t)$. The proof of Theorem 2.1 itself relies on the following two results, connecting the mesh Laplacian operator to the functional Laplace operator and the functional Laplacian to the Laplace-Beltrami operator, respectively.

Theorem 2.3 *Let K be an (ε, η)-approximation of the surface S, and $\varepsilon, \eta < 0.1$. Given a function $f \in C^1(S)$, let $\|f\|_{\infty} = \sup_{x \in S} |f(x)|$, $\|\nabla f\|_{\infty} = \sup_{x \in S} \|\nabla f(x)\|$ and ρ denote the reach of surface S. We have that for any point $w \in S$,*

$$\left| \mathrm{F}_S^h f(w) - \mathrm{L}_K^h(w) \right| \le \frac{\mathrm{Area}(S)}{\pi h^2}$$
$$\left(\left((1 + \frac{2\rho}{\sqrt{h}})\varepsilon + 6\varepsilon\eta + 2\eta^2 \right) \|f\|_{\infty} + \rho\varepsilon \|\nabla f\|_{\infty} \right).$$

Theorem 2.4 (See [8]) *For a function $f \in C^2(S)$, we have that $\lim_{h \to 0} \left\| \mathrm{F}_S^h f(w) - \Delta_S f(w) \right\|_{\infty} = 0$.*

It is easy to see that Theorem 2.1 follows from the two theorems above. Theorem 2.4 was shown in [8], and provides an approximation to the Laplace operator based on heat diffusion. To make it more transparent we give a brief outline of the ideas involved below in Section 2.4. In the remaining of the paper, we focus on the proof of Theorem 2.3. The proof relies on the following result on approximating integrals over a surface, which is of independent interest. Let $d_S(x, y)$ denote the geodesic distance between two points $x, y \in S$.

Theorem 2.5 *Given a Lipschitz function $g : S \to \mathbb{R}$, let $L = \mathrm{Lip}(g)$ be the Lipschitz constant of function g, i.e., $|g(x) - g(y)| \le \mathrm{Lip}(g)d_S(x, y)$. Set $\|g\|_{\infty} = \sup_{x \in S} |g(x)|$. We can approximate $\int_S g d\nu$ by the discrete sum $\mathrm{I}_K g = \sum_{t \in K} \frac{\mathrm{Area}(t)}{\#t} \sum_{v \in V(t)} g(v)$, so that the following inequality holds:*

$$\left| \int_S g d\nu - \mathrm{I}_K g \right| \le 3 \left(\rho L\varepsilon + \|g\|_{\infty} (2\varepsilon + \eta)^2 \right) \mathrm{Area}(S). \quad (5)$$

Moreover, suppose that g is twice differentiable, with the norm of the Hessian of g bounded by H. Then, for some constant C, depending only on S, the following inequality holds:

$$\left| \int_S g d\nu - \mathrm{I}_K g \right| \le \left(CH\varepsilon^2 + 3\|g\|_{\infty} (2\varepsilon + \eta)^2 \right) \mathrm{Area}(S) \quad (6)$$

Note that the second part of the above theorem provides a higher-order approximation, while the first part only requires the function g to be Lipschitz.

Finally, we remark that by using some very recent results on the convergence of Laplace spectrum [2], it can be shown that the discrete eigenfunctions under this framework also converge to eigenfunctions of the Laplace-Beltrami operator of S.

2.4 Functional approximation of the Laplace-Beltrami operator

In this section we attempt to demystify Theorem 2.4 by explaining the underlying idea for the functional approximation of the Laplacian. The core of the approximation theorem lies in the connection of the Laplace-Beltrami operator to the heat equation.

The *heat equation* on the surface S is the partial differential equation

$$\Delta_S u(x, t) = \frac{\partial u}{\partial t}(x, t)$$

The heat equation describes the diffusion of the initial heat distribution $u(x, 0)$ at time t. To obtain an integral approximation for the Laplace operator, we use a functional approximation technique from [7]. The approximation is based on the properties of heat propagation with the initial distribution $u(x, 0) = f(x)$. It is well known (e.g., [20]) that the solution to the heat equation $u(x, t)$ can be written as $u(x, t) = \int_S H_S^t(x, y)f(y)\, d\nu(y)$, where $H_S^t(x, y)$ is the *heat kernel* of the surface S, i.e. the measure of how much heat propagates from x to y in time t. The quantity $\int_S H_S^t(x, y)f(y)\, d\nu(y)$ can be thought of as the sum of all heat coming to point x from every other point y after time t.

Thus the heat equation can be rewritten as follows:

$$\Delta_S u(x, t) = \frac{\partial}{\partial t} \int_S H_S^t(x, y)f(y)\, d\nu(y).$$

Taking the limit as $t \to 0$ and recalling that $u(x,0) = f(x)$ and that $\int H_S^t(x,y)\,d\nu(y) = 1$, yields

$$\Delta_S f(x) = \lim_{t \to 0} \int_S H_S^t(x,y) f(y)\,d\nu(y) =$$

$$\lim_{t \to 0} \frac{1}{t}\left(\int_S H_S^t(x,y) f(y)\,d\nu(y) - f(x)\right) =$$

$$\lim_{t \to 0} \frac{1}{t}\int_S H_S^t(x,y)\,(f(y) - f(x))\,d\nu(y)$$

For the case when S is $\mathbb{R}^N$ the heat kernel can be written explicitly $H_{\mathbb{R}^2}^t(x,y) = \frac{1}{\sqrt{(4\pi t)}}\exp\left(-\frac{\|x-y\|^2}{4t}\right)$, yielding the functional approximation in Eqn (2).

For a general manifold, the heat kernel cannot usually be written explicitly. However the heat kernel can be shown to be close to a Gaussian in the geodesic coordinates (e.g., [20]). By considering the asymptotes of the heat kernel as $t \to 0$, the result in Theorem 2.4 can still be established (see [8]).

3. PROPERTIES OF MESHED SURFACES

In this section, we present several results on the relations between a smooth surface S and an (ε, η)-approximation K of S. For simplicity of the exposition, we assume from now on that K is a triangular mesh. However the same analysis works verbatim for arbitrary (ε, η)-approximation meshes. Let ρ be the reach of S, and $\phi : K \to S$ is the closest-point map introduced in Section 2.2.

3.1   Closeness Between S and K

Given any point $p \in \mathbb{R}^3$, let $d(p, X)$ denote the smallest distance from p to any point in the set $X \subset \mathbb{R}^3$, and n_p the unit normal of S at p. The following result from [6] bounds the surface normal variation between nearby points.

Lemma 3.1 ([6]) *Given two points $p, q \in S$ with $\|p - q\| \leq \rho/3$, the angle between n_p and n_q satisfies that $\angle(n_p, n_q) < \frac{\|p-q\|}{\rho - \|p-q\|}$.*

We will later need the following result bounding the geodesic distance $d_S(p,q)$ between two points $p, q \in S$, in terms of the Euclidean distance $\|p - q\|$. Note that the difference $d_S(p,q) - \|p - q\|$ is of order 3 in $\|p - q\|$, which significantly improves the quadratic bound from [17].

Lemma 3.2 *Given two points $p, q \in S$, let $d = \|p - q\| < \rho/2$. Then we have that $d \leq d_S(p,q) \leq d + \frac{4d^3}{3\rho^2}$.*

Proof: Let γ be the shortest geodesic curve between p and q and set $l = d_S(p,q)$. By Proposition 6.3 in [17] we have that $l \leq 2d$. For any $x \in \gamma$, let $\mathrm{t}_x = \mathrm{t}_x(\gamma)$ be the *unit* tangent vector of γ at x, and $\gamma[p,x]$ the portion of γ from p to x. Set $l_x = d_S(p,x)$.

Since γ is a geodesic, the unit normal of γ at a point $x \in \gamma \subseteq S$ is the same as the unit surface normal n_x at x, and the curvature of γ is upper bounded by $1/\rho$. It then follows from the Frenet Formulas that $\|dt_x/dl_x\| \leq \|n_x/\rho\| = 1/\rho$. Hence we have that

$$\|t_x - t_p\| = \left\|\int_{\gamma[p,x]} dt_y\right\| \leq \int_{\gamma[p,x]} \frac{1}{\rho}\,dl_y \leq \frac{l_x}{\rho}$$

$$\Rightarrow \quad \sin\frac{\angle(\mathrm{t}_p, \mathrm{t}_x)}{2} \leq \frac{l_x}{2\rho}.$$

Furthermore, let $u \cdot v$ denote the dot-product between vectors u and v. Then we have that

$$\int_\gamma t_x \cdot t_p\,dl_x = \int_\gamma \cos\angle(t_x, t_p)\,dl_x = \int_\gamma \left(1 - 2\sin^2\frac{\angle(t_x, t_p)}{2}\right)dl_x$$

$$\geq \int_\gamma \left(1 - \frac{l_x^2}{2\rho^2}\right)dl_x = l - \frac{l^3}{6\rho^2}$$

On the other hand, observe that $\int_\gamma t_x \cdot t_p\,dl_x$ measures the length of the (signed) projection of γ along the direction t_p. That is,

$$\int_\gamma t_x \cdot t_p\,dl_x = (q - p)\cdot t_p.$$

Hence we have that

$$d = \|p - q\| \geq (q - p)\cdot t_p \geq l - \frac{l^3}{6\rho^2}$$

$$\Rightarrow \quad l \leq d + \frac{l^3}{6\rho^2} \leq d + \frac{4d^3}{3\rho^2}.$$

The last inequality follows from the fact that $l \leq 2d$. This proves the lemma. ∎

Lemma 3.3 *If a mesh K (ε, η)-approximates S with $\varepsilon, \eta < 0.1$ then the following conditions hold:*

  (i) For any point $k \in K$, $d(k, S) \leq (\varepsilon^2 + \varepsilon\eta)\rho$.

  (ii) For any point $x \in S$, $d(x, K) \leq (\varepsilon^2 + \varepsilon\eta)\rho$.

  (iii) $\phi : K \to S$ is a homeomorphism.

Proof: To show (i), consider the figure on the right. Suppose the point k is contained in the triangle $t \in K$ and p is any vertex of t. Let T_p denote the tangent plane at p. Assume that B and B' are the two balls of radius ρ tangentially touching S at p on each side of T_p, and the centers of B and B' are o and o', respectively.
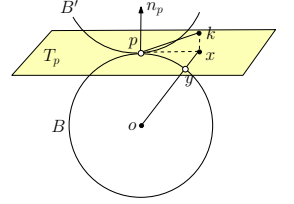
Recall that n_t is the normal of the triangle t and n_p is the unit surface normal of S at p. Since $\angle(n_p, n_t) < \eta$, the angle between T_p and the plane passing through t is smaller than η, implying that the angle between T_p and the line passing through pk is at most η. Let x denote the projection of k on T_p. We have that

$$\|x - p\| \leq \|k - p\| \leq \varepsilon\rho, \quad \text{and}$$

$$\|k - x\| \leq \|p - k\|\sin\eta \leq \varepsilon\eta\rho.$$

Furthermore, observe that one of the segments xo and xo' must intersect S. Assume without loss of generality that it is xo. Since B does not contain any point from S, we have that $d(x, S) \leq \|x - y\|$ where y is the intersection between xo and B. This implies that

$$d(x, S) \leq \sqrt{\rho^2 + \|x - p\|^2} - \rho \leq \varepsilon^2\rho.$$

Since $d(k, S) \leq \|k - x\| + d(x, S)$ by the triangle inequality, Part (i) then follows.

We now show claim (iii), and claim (ii) follows easily from (i) and (iii). Note that by (i), K does not intersect the medial axis of S. Hence the map ϕ is well-defined and actually continuous. Since K is compact, to show (iii), it suffices to show that ϕ is bijective.

First, assume that ϕ is not injective, and it maps two points $k, k' \in K$ to the same point, say $x \in S$. In this case, both k and k' are on the line l passing through x in direction n_x. Without loss of generality, assume that k and k' are two consecutive intersection points between l and K. Let t and t' be the triangles that contain k and k', respectively. See the right figure for an example. By (i), we have that both $\|k - x\|$ and $\|k' - x\|$ are upper-bounded by $(\varepsilon^2 + \varepsilon\eta)\rho$.
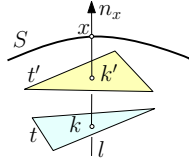
Consider any vertex p of t. We have that $\|x - p\| \le \|x - k\| + \|k - p\| \le (\varepsilon + \varepsilon^2 + \varepsilon\eta)\rho$, by triangle inequality. Since both x and p are in S, we have that $\angle(n_x, n_p) \le 2\varepsilon$ by Lemma 3.1. It then follows that

$$\angle(n_x, n_t) \text{ and } \angle(n_x, n_{t'}) \le 2\varepsilon + \eta . \tag{7}$$

The above equation implies that $t \ne t'$, as otherwise, l lies in the plane passing through t and as such $\angle(n_x, n_t) = \pi/2$, which is not possible. Since k and k' are two consecutive intersection points between L and K, n_x must point to the inside of K at one of these two points, say k. If k lies in the interior of t, then $\angle(n_x, n_t) \ge \pi/2$. Otherwise, k is on the boundary of t, in which case $\angle(n_x, n_t) \ge \pi/2 - 2\eta$ because it follows from the definition of (ε, η)-approximation that the neighboring triangle of t forms an angle of at most 2η with t. Either case contradicts Eqn (7) since $\varepsilon, \eta < 0.1$ by hypothesis. Hence we cannot have two such points k and k' and the map ϕ must be injective.

Finally, note that the image of K under the map ϕ, $\phi(K) \subseteq S$, is a compact surface as well. Since S is connected, by Theorem (7.6) [18], $\phi(K) = S$. It then follows that $\phi : K \to S$ is a homeomorphism. ∎

3.2 Approximating Integrals on the Surface S

Lemma 3.3 implies that the mesh K is close to the underlying surface S both geometrically and topologically. Intuitively, quantities defined on S are closely related to their analogs defined on K (i.e, the pre-images under ϕ). Indeed, consider an arbitrary but fixed triangle $t \in K$. Note that although the map ϕ is not differentiable on the entire domain K, its restriction to the interior of t is differentiable. We now present a result (Lemma 3.5) which states that $J(x)$, the *Jacobian* of the map ϕ at an interior point $x \in t$, is close to 1. First, for any point $x \in t$, let $\hat{n}_x$ be the surface normal at $\phi(x)$; that is, $\hat{n}_x = n_{\phi(x)}$. We need the following lemma from [6], saying that the rate that $\hat{n}_x$ changes as x moves around in t is bounded.

Lemma 3.4 *Let K be a triangular mesh that (ε, η)-approximates S with $\varepsilon, \eta < 0.1$. Given any triangle $t \in K$, for any x in the interior of t, and for any unit vector v in the plane passing through t, we have that*

$$\left| \lim_{\delta \to 0} \frac{\angle(\hat{n}_{x + \delta v}, \hat{n}_x)}{\delta} \right| \le \frac{1}{(1 - \varepsilon)\rho} ,$$

We now present our result on bounding the Jacobian of the map ϕ. Note that by a nice differential geometric argument, Morvan and Thibert [16] and Hildebrandt *et. al.* [13] analyze the Jacobian of ϕ when the meshed surface K is close to S under the Hausdorff distance and normal variation. A bound similar to that in Lemma 3.5 can be derived by combining Lemma 3.3 with their results. For completeness of the exposition we include an elementary geometric proof here.

Lemma 3.5 *Let K be a triangular mesh that (ε, η)-approximates S with $\varepsilon, \eta < 0.1$. For any point x in the interior of an arbitrary triangle $t \in K$, we have that $|J(x) - 1| \le 2(2\varepsilon + \eta)^2$. In particular, this implies that the areas of S and K satisfies:*

$$\left| \frac{\text{Area}(S)}{\text{Area}(K)} - 1 \right| \le 2(2\varepsilon + \eta)^2.$$

Proof: Let P be the plane where the triangle t lies, and $T_{\phi(x)}$ be the tangent plane of S at $\phi(x)$. Set α denote the angle between the planes P and $T_{\phi(x)}$. Note that $\alpha < 2\varepsilon + \eta$ by Eqn (7). Easy to see that there exists an orthogonal coordinate system (u, v) on P such that $\angle(u, T_{\phi(x)}) = \alpha$ and $\angle(v, T_{\phi(x)}) = 0$. Let $\phi_u(x)$ and $\phi_v(x)$ be the partial derivatives of ϕ at a point $x = (u_0, v_0)$ in the interior of t, respectively. The Jacobian $J(x) = J(u_0, v_0)$ of ϕ at x then equals $\sqrt{EG - F^2}$, where $E = \phi_u \cdot \phi_u$, $G = \phi_v \cdot \phi_v$ and $F = \phi_u \cdot \phi_v$.

To bound ϕ_u, consider the point $y = (u_0 + \delta, v_0)$, where δ is a real number. Note that by the choice of the direction u, the angle $\angle((y - x), T_{\phi(x)})$ between $y - x$ and the plane $T_{\phi(x)}$ is α. Let z be the projection point of y onto $T_{\phi(x)}$ and b be the projection of $\phi(y)$ onto the line yz. See the right figure. Set $\theta = \angle(\hat{n}_x, \hat{n}_y)$; note that $\theta \le \frac{\delta}{(1 - \varepsilon)\rho}$ by Lemma 3.4. Since $\|\phi(y) - y\| \le (\varepsilon^2 + \varepsilon\eta)\rho$ by Lemma 3.3, we have that
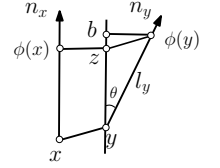
$$\|\phi(y) - b\| = \|\phi(y) - y\| \cos\theta < \frac{\varepsilon^2 + \varepsilon\eta}{1 - \varepsilon} |\delta|$$

Now let B and B' be the two balls of radius ρ that tangentially touch S at $\phi(x)$. By the definition of the reach ρ, the surface S has to lie outside these two balls.

First we show $\|z - b\|$ is of order δ^2. Let z' be the projection of $\phi(y)$ onto $T_{\phi(x)}$; $\|z - z'\| = \|\phi(y) - b\|$ is of order δ. Hence by triangle inequality,

$$\|\phi(x) - z'\| \le \|\phi(x) - z\| + \|z - z'\|$$

is of order δ. Furthermore, since $\phi(y)$ has to lie in between B and B', we can show that $\|\phi(y) - z'\|$, thus $\|z - b\|$, is of order δ^2. Hence we have that:

$$\lim_{\delta \to 0} \frac{\|z - \phi(y)\|}{|\delta|} \le \lim_{\delta \to 0} \frac{\|z - b\| + \|b - \phi(y)\|}{|\delta|}$$
$$\le \frac{\varepsilon^2 + \varepsilon\eta}{1 - \varepsilon} \tag{8}$$

By definition, $\sqrt{E} = \lim_{\delta \to 0} \frac{\|\phi(x) - \phi(y)\|}{|\delta|}$. Consider the triangle consisting of $\phi(x), \phi(y)$ and z. Since
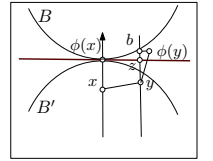
$$\|\phi(x) - z\| = \|y - x\| = \delta \cos\alpha,$$

it follows from the triangle inequality and Eqn (8) that

$$|\sqrt{E} - 1| \le (1 - \cos\alpha) + \frac{\varepsilon^2 + \varepsilon\eta}{1 - \varepsilon}.$$

Furthermore, let α_u be the angle between the vectors $z - \phi(x)$ and ϕ_u (i.e, $\phi(y) - \phi(x)$). We have for small enough δ that

$$\sin\alpha_u \le \frac{\|z - \phi(y)\|}{\|z - \phi(x)\|} \le \frac{\varepsilon^2 + \varepsilon\eta}{(1 - \varepsilon)\cos\alpha}.$$

Similarly, let $w = (u_0, v_0 + \delta)$ and z' the projection of w onto the plane $T_{\phi(x)}$. Let $\alpha_v = \angle((z' - \phi(x)), \phi_v)$. Similar argument can

show that

$$|\sqrt{G} - 1| \;\leq\; \frac{\varepsilon^2 + \varepsilon\eta}{1 - \varepsilon} \quad \text{and}$$

$$\sin\alpha_v \;\leq\; \frac{\|z - \phi(y)\|}{\|z - \phi(x)\|} \;\leq\; \frac{\varepsilon^2 + \varepsilon\eta}{(1 - \varepsilon)}.$$

Finally, observe that by the triangle inequality,

$$|\angle(\phi_u, \phi_v) - \pi/2| \;\leq\; (\alpha_u + \alpha_v).$$

Since $|F| = \sqrt{EG}|\cos\angle(\phi_u, \phi_v)|$, it follows that

$$\sqrt{EG}\,(1 - \cos^2\angle(\phi_u, \phi_v)) \;\leq\; \sqrt{EG - F^2} \;\leq\; \sqrt{EG}$$

and the lemma follows from the bounds derived for E, G, a_u, a_v.
∎

3.3 Proof of Theorem 2.5

We now prove one of our main results on approximating integral on a meshed surface. Let $g : S \to \mathbb{R}$ be a function defined on S. We wish to approximate the integral $\int_S g(x)\,d\nu(x)$ using the values $g(v)$ at vertices v of the mesh K. Specifically, we construct a discrete version of the integral $\int_S g\,d\nu$ by setting $\mathrm{I}_K g = \sum_{t \in K} \frac{\mathrm{Area}(t)}{\#t} \sum_{v \in V(t)} g(v)$, where $\#t$ is the number of vertices in the face t (3 for a triangulation). Each face of the mesh contributes the amount equal to its area multiplied by the average value of its vertices. It can be shown that, for a triangular mesh, the above discretization of the integral is the same as the one obtained by intepolating a function g linearly on each triangle.

First part of Theorem 2.5. We prove Theorem 2.5 via the map ϕ. Since ϕ is a homeomorphism, the set of surface mesh faces $\{\phi(t), t \in K\}$ partitions the surface S. Therefore from the change of variable formula we have

$$\int_S g(x)\,d\nu(x) = \sum_{t \in K} \int_{\phi(t)} g(x)\,d\nu(x)$$
$$= \sum_{t \in K} \int_t g(\phi(u,v))\mathrm{J}(u,v)\,du\,dv\,,$$

where (u, v) is any orthogonal coordinate system on the plane passing through the face t. It then follows from Lemma 3.5 that

$$\left| \int_S g(x)\,d\nu(x) - \sum_{t \in K} \int_t g(\phi(u,v))\,dudv \right|$$
$$\leq \left| \sum_{t \in K} \int_t g(\phi(u,v)) 2(2\varepsilon + \eta)^2\,dudv \right| \qquad (9)$$
$$\leq 2(2\varepsilon + \eta)^2 \mathrm{Area}(K)\|g\|_\infty$$

On the other hand, for any vertex p of t and any point $x = (u, v) \in t$, we have that $\|p - x\| \leq \varepsilon\rho$ by definition of (ε, η)-approximation. It then follows from Lemma 3.3 (i) and the triangle inequality that

$$\|p - \phi(x)\| \leq (\varepsilon + \varepsilon^2 + \varepsilon\eta)\rho.$$

Since $\varepsilon, \eta < 0.1$, we have that $d_S(p, \phi(x)) \leq 2\varepsilon\rho$ by Lemma 3.2. Therefore

$$|g(\phi(x)) - g(p)| \leq 2\rho L\varepsilon,$$

where $L = \mathrm{Lip}(g)$ is the Lipschitz constant of g. This implies that

$$\left| \int_t g(\phi(u,v)) - g(p)\,dudv \right| \leq 2\rho L\varepsilon \mathrm{Area}(t).$$

Combining it with Eqn (9) and noticing that p is an arbitrary vertex of t, we have that

$$\left| \int_S g\,d\nu - \mathrm{I}_K g \right| \leq 2\rho L\varepsilon \mathrm{Area}(K) + 2(2\varepsilon + \eta)^2 \mathrm{Area}(K)\|g\|_\infty$$

Since by Lemma 3.5, we have that $\mathrm{Area}(K) \leq 1.5\mathrm{Area}(S)$. This thus proves the first part of Theorem 2.5.

Second part of Theorem 2.5. In the case when we have a triangular mesh and the function g is twice differentiable, this analysis can be improved to show higher-order convergence. Below we provide a sketch of the proof.

Consider a twice-differentiable function $h : t \to \mathbb{R}$ on a triangle $t \in K$, and let p, q, r be the vertices of t. As above, let $x = (u, v)$ be an orthonormal coordinate system on the plane of t. Consider the unique linear function $l(x)$ defined on the plane of the triangle, s.t. $l(p) = h(p), l(q) = h(q), l(r) = h(r)$. The first observation is that [1]

$$\int_t l(u,v)dudv = \frac{1}{3}(h(p) + h(q) + h(r))\mathrm{Area}(t).$$

Now without loss of generality assume that p is the origin O of the coordinate system and that $h(p) = 0$ (additive constants will not change the computation). Let $q = (u_1, v_1), r = (u_2, v_2)$. Since l is a linear function, straightforward calculations show that

$$l(u,v) = (u \;\; v) \begin{pmatrix} u_1 & v_1 \\ u_2 & v_2 \end{pmatrix}^{-1} \begin{pmatrix} h(q) \\ h(r) \end{pmatrix}. \qquad (10)$$

Writing the Taylor expansion for h with a quadratic remainder term, and recalling that $h(0) = 0$, we have that

$$|h(u,v) - h_u(0)u - h_v(0)v| < H(u^2 + v^2),$$

where H is maximum of the norm of the Hessian of h on the triangle, and h_u (resp. h_v) is the partial derivative of h along u (resp. v). Now based on the observation that the function value of a linear function inside a triangle is bounded by the sum of its (absolute) values on the vertices, and that the length of each side of t is at most $\varepsilon\rho$, it can be shown that

$$|l(u,v) - h_u(0)u - h_v(0)v| \;\leq\; 4H(\varepsilon\rho)^2.$$

Combining this with Eqn (10) leads to that

$$|h(u,v) - l(u,v)| < 5H(\varepsilon\rho)^2.$$

Finally, set $h(x) = g(\phi(u,v))$. Note that ϕ is infinitely differentiable outside of the medial axis. Thus by a standard compactness argument, the second derivative of ϕ, and thus of $g(\phi(x, y))$ (from the chain rule), is bounded. Hence

$$|g(u,v) - l(u,v)| < CH\varepsilon^2,$$

where C is some constant depending on the geometry of S. Integrating, and using Eqn (9) we obtain

$$\left| \int_S g\,d\nu - \mathrm{I}_K g \right| \;\leq\; CH\varepsilon^2 \mathrm{Area}(K) + 2(2\varepsilon + \eta)^2 \mathrm{Area}(K)\|g\|_\infty$$

[1] We remark that this implies that, for a triangular mesh, we have $\mathrm{I}_K g = \int \hat{g}$, where the integral is taken over the mesh (considered as a piece-wise linear manifold) and $\hat{g}$ is a (unique) piece-wise function obtained by linearly interpolating the values of g on vertices of each triangle t to the interior of t.

Since $\mathrm{Area}(K) \leq 1.5\mathrm{Area}(S)$, the second part of Theorem 2.5 then follows.

4. DISCRETE LAPLACE OPERATOR

We now show our main result (Theorem 2.1) which states that the mesh Laplacian approximates the surface Laplacian well. We first prove Theorem 2.3; that is, given a mesh K (ε, η)-approximating a surface S, for any point $w \in S$, the difference between the mesh and the functional Laplace operators $|\mathrm{F}_S^h f(w) - \mathrm{L}_K^h(w)|$ is bounded, and converges to zero as ε and η go to 0. Theorem 2.1 then follows from this theorem and Theorem 2.4.

Proof of Theorem 2.3. First, set $g(x) = \frac{1}{4\pi h^2} e^{-\frac{\|x-w\|^2}{4h}} (f(x) - f(w))$. Comparing Eqn (2) and Eqn (1), we obtain that

$$\left| \mathrm{L}_K^h f(w) - \mathrm{F}_S^h f(w) \right| = \left| \int_S g d\nu - \mathrm{I}_K g \right| \quad (11)$$

By (the first part of) Theorem 2.5, to bound the above quantity, it suffices to bound $\|g\|_\infty$ and the Lipschitz constant $\mathrm{Lip}(g)$ of g. Easy to verify that $\|g\|_\infty \leq \frac{1}{2\pi h^2} \|f\|_\infty$. For $\mathrm{Lip}(g)$, since f, and thus g, is C^1-continuous, it is upper bounded by $\|g'\|_\infty = \sup_{x \in S} \|g'(x)\|$. Notice that $g'(x)$ is a map from the tangent space T_x to $\mathbb{R}$. By definition, $g'(x)(v) = \nabla_S g(x) \cdot v$ for any vector $v \in T_x$ and hence $\|g'(x)\| = \|\nabla_S g(x)\|$. On the other hand, it is easy to verify that

$$\|\nabla_S g(x)\| \leq \frac{1}{4\pi h^2} (2\|f\|_\infty \cdot \|\nabla_S e^{-\frac{\|x-w\|^2}{4h}}\| + \|\nabla_S f(x)\|).$$

Since S is a surface embedded in $\mathbb{R}^3$ with the induced Riemannian metric, it holds that

$$\|\nabla_S e^{-\frac{\|x-w\|^2}{4h}}\| \leq \|\nabla_{\mathbb{R}^3} e^{-\frac{\|x-w\|^2}{4h}}\|$$
$$= e^{-\frac{\|x-w\|^2}{4h}} \|x-w\|/(2h) \leq \frac{1}{\sqrt{h}},$$

where the last inequality holds as $y/e^{y^2} \leq 1$ for any real number y. It then follows that

$$\|g'\|_\infty = \|\nabla_S g(x)\| \leq \frac{1}{4\pi h^2} \left(\frac{2\|f\|_\infty}{\sqrt{h}} + \|f'\|_\infty \right).$$

Combining with Theorem 2.5, and putting everything together, we conclude with Theorem 2.3.

Proof of Theorem 2.1. Now let $K_{\varepsilon, \eta}$ denote an (ε, η)-approximation of S with $\varepsilon, \eta < 0.1$, and $h(\varepsilon, \eta)$ an appropriate constant depending on ε and η. We have that for any point $w \in S$,

$$\left| \mathrm{L}_{K_{\varepsilon,\eta}}^{h(\varepsilon,\eta)} f(w) - \Delta_S f(w) \right| \leq \left| \mathrm{L}_{K_{\varepsilon,\eta}}^{h(\varepsilon,\eta)} f(w) - \mathrm{F}_S^{h(\varepsilon,\eta)} f(w) \right|$$
$$+ \left| \mathrm{F}_S^{h(\varepsilon,\eta)} f(w) - \Delta_S f(w) \right|.$$

By choosing $h(\varepsilon, \eta) = \varepsilon^{\frac{1}{2.5+\alpha}} + \eta^{\frac{1}{1+\alpha}}$, where $\alpha > 0$ is an arbitrary fixed positive number, it follows from Theorem 2.3 that

$$\left| \mathrm{L}_{K_{\varepsilon,\eta}}^{h(\varepsilon,\eta)} f(w) - \Delta_S f(w) \right| \leq O(\varepsilon^{\frac{\alpha}{2.5+\alpha}}) + O(\eta^{\frac{\alpha}{1+\alpha}})$$
$$+ |\mathrm{F}_S^{h(\varepsilon,\eta)} f(w) - \Delta_S f(w)|$$

The big-O notation above hides terms linear in the area $\mathrm{Area}(S)$, the reach $\rho(S)$, $\|f\|_\infty$ and $\|f'\|_\infty$. On the other hand, the limit $\lim_{t \to 0} |\mathrm{F}_S^{h(\varepsilon,\eta)} f(w) - \Delta_S f(w)| = 0$ by Theorem 2.4([8]). Hence by taking the limit, we see that $\lim_{\varepsilon, \eta \to 0} \mathrm{L}_{K_{\varepsilon,\eta}}^{h(\varepsilon,\eta)} f(w) = \Delta_S f(w)$, which proves Theorem 2.1.

5. EXPERIMENTS

In this section, we apply our algorithm of computing the mesh Laplacian to different surfaces and show its convergence as the mesh becomes finer. One currently widely used mesh Laplace operator is the *cotangent* (COT)*n scheme*, originally proposed by Pinkall and Polthier [19]. We compare our algorithm with its modified version [15, 25], which produces better results than the original method. Our experiments show that the COT scheme does not produce convergence for functions other than linear functions, while our method, in addition to exhibiting convergence behavior, is also much more robust with respect to noisy data.

Experimental setup. To analyze the convergence behavior, we need the "ground truth", that is, we need to know the Laplace-Beltrami operator for the underlying surface approximated by input meshes. This somewhat limits the type of surfaces that we can experiment with. In this paper, we consider two types of surfaces: planar surfaces and spherical surfaces.

For the planar surface, we uniformly sample the region $[-1, 1] \times [-1, 1]$ with different density, and construct the Delaunay triangulation for the resulting sample points. For the spherical surface, we sample a unit sphere, either uniformly or non-uniformly, with different density, and then use the COCONE software [5] to generate the triangular meshes. The goal of the non-uniform sampling is to create "bad" meshes, such as those with skinny triangles and triangles of different sizes. We also produce noisy data from the uniform sampling of the sphere, by perturbing each sample point randomly by a small shift. Some examples of these three types of spherical meshes are shown in Figure 1.
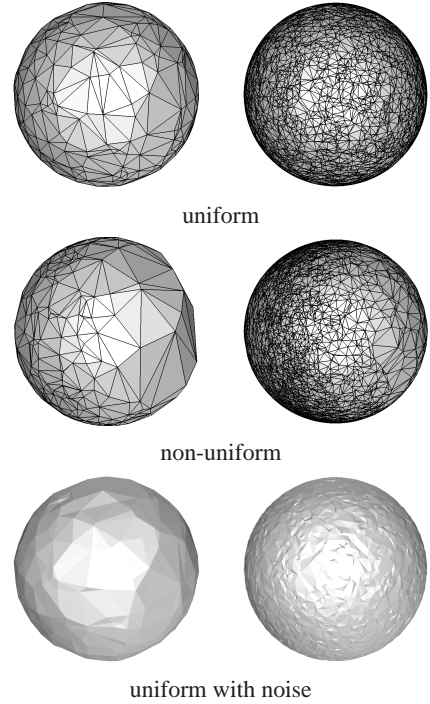

uniform

non-uniform

uniform with noise

Figure 1: Meshes for spherical surface with 500 sample points and 8000 sample points.

Error measure. Given a mesh K approximating a surface S and an input function $f : S \to \mathbb{R}$, we evaluate the surface Laplacian and the mesh Laplacian at each of the n vertices of K, and obtain

two n dimensional vectors U and $\widehat{U}$, respectively. To measure the error between the mesh Laplacian and the surface Laplacian, we consider the commonly used normalized L_2 error $E_2 = \frac{\|U - \widehat{U}\|_2}{\|U\|_2}$. We remark that our theoretical result is that our mesh Laplacian converges under the L_∞ *norm* (i.e, point-wise convergence), which is a stronger result than the L_2-*convergence* (as L_∞-convergence implies L_2-convergence for compact spaces). Such convergence is indeed observed for all types of meshes that we have conducted experiments on. However, since the COT scheme does not show any convergence under the L_∞ error metric, we will mainly show results under the L_2 error metric from now on — our method compares even more favorably under the L_∞ error. We will show results under the L_∞ error for one data set (Table 3), and the performances over other data sets are similar.

Results for planar surface. Given a function $f : \mathbb{R}^2 \to \mathbb{R}$ on the plane, its surface Laplacian is simply: $\Delta_{\mathbb{R}^2} f(x, y) = \frac{\partial^2 f}{\partial x^2} + \frac{\partial^2 f}{\partial y^2}$. Specifically, $\Delta_{\mathbb{R}^2} f(x, y) = 0$ if f is a linear function. It turns out that the COT scheme produces exactly 0 for a linear function on a planar mesh. Hence we compare the mesh Laplacians for two non-linear functions: $f(x, y) = x^2$ and $f(x, y) = e^{x+y}$. The results under the normalized L_2 error metric are shown in Table 1. For both functions, for different values of the parameter h, our method always presents convergence behavior; while finer mesh does not lead to lower approximation error by the COT scheme. Note that we obtain better approximation even when the number of sample points is small (500). Since different values of h show similar behavior, from now on, we fix the parameter at $4h = 0.04$.

Method	Param	500	2000	8000	16000
COT	non	0.220	0.173	0.197	0.207
OUR	4h=0.01	0.450	0.146	0.040	0.022
	4h=0.04	0.126	0.038	0.010	0.005
	4h=0.09	0.069	0.017	0.004	0.002
$f = x^2$					
COT	non	0.198	0.188	0.190	0.202
OUR	4h=0.01	0.875	0.128	0.055	0.027
	4h=0.04	0.189	0.037	0.022	0.016
	4h=0.09	0.099	0.033	0.027	0.025
$f = exp(x + y)$					

Table 1: Normalized L_2 error for planar mesh. We show the results of our method with there different h values.

Spherical surfaces. Given a function $f : \mathbb{S}^2 \to \mathbb{R}$ defined on the unit sphere $\mathbb{S}^2$, where f is parametrized by the spherical coordinates θ and ϕ, its spherical surface Laplacian is:

$$\Delta_{\mathbb{S}^2} f(\theta, \phi) = \frac{1}{\sin\theta} \frac{\partial}{\partial\theta}\left(\sin\theta \frac{\partial f}{\partial\theta}\right) + \frac{1}{\sin^2\theta} \frac{\partial^2 f}{\partial\phi^2}.$$

Xu [25] proved that his modification of the COT scheme can produce convergent result for linear function defined on spheres. Indeed, this is observed in our experimental results as shown in Table 2, where we also compare the mesh Laplacians for two non-linear functions $f(x, y, z) = x^2$ and $f(x, y, z) = e^x$ for a uniformly sampled spherical mesh. However, while our method converges for all the three functions, the COT scheme only converges under the linear function. In Table 3, we also show the approximation error of the two mesh Laplacians under the L_∞ error metric. Note that compared to the case of normalized L_2 error, the numerical values of L_∞ error can be big, as it is the absolute error and not normalized.

We also test the COT scheme and our mesh Laplacian for meshes

Method	500	2000	8000	16000
COT	0.058	0.030	0.015	0.011
OUR	0.606	0.142	0.034	0.017
$f = x$				
COT	0.171	0.157	0.158	0.155
OUR	0.488	0.115	0.013	0.005
$f = x^2$				
COT	0.124	0.101	0.102	0.099
OUR	0.613	0.140	0.028	0.015
$f = \exp(x)$				

Table 2: Normalized L_2 error for spherical meshes with uniform sampling.

Method	500	2000	8000	16000
COT	0.229	0.185	0.083	0.062
OUR	2.097	0.492	0.081	0.037
$f = x$				
COT	1.147	1.577	1.478	1.375
OUR	2.915	0.838	0.062	0.025
$f = x^2$				
COT	0.798	0.887	0.928	0.849
OUR	4.000	0.873	0.112	0.054
$f = \exp(x)$				

Table 3: Normalized L_∞ error for spherical meshes with uniform sampling.

constructed from points non-uniformly sampled from the unit sphere. The error obtained for both methods are fairly similar to that on the regular mesh (as reported in Tables 2 and 3).

Finally, in Table 4, we show how our method and the COT scheme perform for noisy data. Note that even though the COT scheme has been proven to converge for linear functions on a sphere, once the mesh becomes noisy, such convergence behavior is lost; while the approximation error by our algorithm stays almost the same as before. This is not too surprising as our scheme considers a much larger neighborhood than COT scheme when evaluating the mesh Laplacian at a point, which has the "smoothing" effect. However, it is not clear how to extend COT scheme to incorporate larger neighborhood than its current one-ring neighborhood.

Method	500	2000	8000	16000
COT	0.398	1.532	3.015	0.936
OUR	0.599	0.155	0.051	0.022
$f = x$				
COT	0.267	0.914	1.840	0.545
OUR	0.484	0.128	0.028	0.006
$f = x^2$				
COT	0.308	1.271	2.631	0.817
OUR	0.612	0.153	0.043	0.018
$f = \exp(x)$				

Table 4: Normalized L_2 error for the experiments on the sphere with noise.

Remark. Finally, we remark that we have also compared our mesh Laplacian with the graph Laplacian. Graph Laplacian has been shown to converge for *points randomly sampled from the uniform distribution on the underlying manifold* [8], which is also observed in our experiments when points are randomly sampled. However, our mesh Laplacian produces consistently smaller errors. For non-uniformly sampled meshes, graph Laplacian is not expected to converge to the surface Laplacian.

6. CONCLUSIONS

In this paper, we have developed the first algorithm for approximating the Laplace operator on a meshed surface with point-wise convergence guarantee. Such convergence is required in many applications, where quantities, such as mean curvature, need to be estimated at each node of the mesh. The convergence result does not require the aspect ratio of mesh elements to be bounded. Experimental results show that our algorithm indeed exhibits convergence empirically, and outperforms current popular methods both in accuracy and in its robustness with respect to noisy data. To provide theoretical analysis of our algorithm, we also established a general result to compare integrals over a smooth surface and their discretization on a mesh.

In conclusion we would like to make several points about different aspects of our algorithm and future directions.

Adaptivity. The algorithm as stated can be easily adapted to the size of the mesh. For example a sensible heuristic is to take h to be a multiple (say, 3) of the average edge length at a point. However, our analysis is not yet adapted to the local feature size. It seems promising to develop a version of Theorem 2.3 and Theorem 2.5 using the local feature size. It may be more difficult to develop an adaptive version of Theorem 2.4 as somewhat subtle analysis of the heat kernel on a surface may be needed.

Higher dimensions. The algorithms in this paper can be straightforwardly modified to work with high dimensional meshes or simplicial complexes. It seems that the analogues of Theorem 2.5 and Theorem 2.1 will hold. However the exact conditions are likely to be different and the proofs may need to be significantly modified.

Orientability and boundary. The orientability condition and no-boundary condition, although necessary for our current proofs, seems to be not essential. One future direction is to extend our results to non-orientable surfaces and/or surfaces with boundary. Note that our current results hold for interior points of a surface with boundary.

Noisy data. Due to the averaging nature of the mesh Laplacian, the method seems to demonstrate good stability with respect to noise in the input mesh, as shown in our experiments. However, theoretical analysis for this case still needs to be developed.

Point clouds. Another future direction is the analysis of point clouds, where no mesh is given. A particular interesting case is when intrinsic dimension of the manifold is much small than the dimension of the ambient space, and we wish that our algorithm depends on the intrinsic dimension. This direction seems to have interesting connection with the body of work on surface reconstruction (see, e.g. [11]). We note that [7] also deals with reconstructing the Laplace operator from point clouds. However the probabilistic nature of data in machine learning allows one to use large deviations methods, while in surface reconstruction, the probabilistic assumption cannot usually be made.

7. REFERENCES

[1] Discrete differential geometry: An applied introduction. SIGGRAPH 2005 / 2006 course notes.

[2] Convergence of Laplacian Eigenmaps. Preprint, 2008.

[3] P. Alliez, M. Meyer, and M. Desbrun. Interactive geometry remeshing. In *SIGGRAPH '02: Proceedings of the 29th annual conference on Computer graphics and interactive techniques*, pages 347–354, New York, NY, USA, 2002. ACM Press.

[4] N. Amenta and M. Bern. Surface reconstruction by voronoi filtering. *Discr. Comput. Geom.*, 22:481–504, 1999.

[5] N. Amenta, S. Choi, T. K. Dey, and N. Leekha. A simple algorithm for homeomorphic surface reconstruction. *Internat. J. Comput. Geom. & Applications*, 12:125–141, 2002.

[6] N. Amenta and T. K. Dey. Normal variation with adaptive feature size. *http://www.cse.ohio-state.edu/~tamaldey/papers.html*, 2007.

[7] M. Belkin and P. Niyogi. Laplacian eigenmaps for dimensionality reduction and data representation. *Neural Computation*, 15(6):1373–1396, 2003.

[8] M. Belkin and P. Niyogi. Towards a theoretical foundation for laplacian-based manifold methods. In *COLT*, pages 486–500, 2005.

[9] L. Demanet. Painless, highly accurate discretizations of the laplacian on a smooth manifold. Technical report, Stanford University, 2006.

[10] M. Desbrun, M. Meyer, P. Schröder, and A. H. Barr. Implicit fairing of irregular meshes using diffusion and curvature flow. *Computer Graphics*, 33(Annual Conference Series):317–324, 1999.

[11] T. K. Dey. *Curve and Surface Reconstruction: Algorithms with Mathematical Analysis (Cambridge Monographs on Applied and Computational Mathematics)*. Cambridge University Press, New York, NY, USA, 2006.

[12] S. Dong, P.-T. Bremer, M. Garland, V. Pascucci, and J. C. Hart. Spectral surface quadrangulation. In *SIGGRAPH '06: ACM SIGGRAPH 2006 Papers*, pages 1057–1066, New York, NY, USA, 2006. ACM Press.

[13] K. Hildebrandt, K. Polthier, and M. Wardetzky. On the convergence of metric and geometric properties of polyhedral surfaces. *Geometriae Dedicata*, 123(1):89–112, December 2006.

[14] U. F. Mayer. Numerical solutions for the surface diffusion flow in three space dimensions. *comput. Appl. Math*, 20(3):361–379, 2001.

[15] M. Meyer, M. Desbrun, P. Schröder, and A. H. Barr. Discrete differential geometry operators for triangulated 2-manifolds. In *Proc. VisMath'02*, Berlin, Germany, 2002.

[16] J.-M. Morvan and B. Thibert. Approximation of the normal vector field and the area of a smooth surface. *Discrete & Computational Geometry*, 32(3):383–400, 2004.

[17] P. Niyogi, S. Smale, and S. Weinberger. Finding the homology of submanifolds with high confidence from random samples. *Discrete and Computational Geometry*, 2006.

[18] B. O'Neil. *Elementary Differential Geometry*. Academic Press, New York, NY, USA, 1966.

[19] U. Pinkall and K. Polthier. Computing discrete minimal surfaces and their conjugates. *Experimental Mathematics*, 2(1):15–36, 1993.

[20] S. Rosenberg. *The Laplacian on a Riemannian Manifold: An Introduction to Analysis on Manifolds*. Cambridge University Press, 1997.

[21] O. Sorkine. Differential representations for mesh processing. *Computer Graphics Forum*, 25(4):789–807, 2006.

[22] O. Sorkine, Y. Lipman, D. Cohen-Or, M. Alexa, C. Rössl, and H.-P. Seidel. Laplacian surface editing. In *Proceedings of the Eurographics/ACM SIGGRAPH Symposium on Geometry Processing*, pages 179–188. ACM Press, 2004.

[23] G. Taubin. A signal processing approach to fair surface design. In *SIGGRAPH '95: Proceedings of the 22nd annual conference on Computer graphics and interactive techniques*, pages 351–358, New York, NY, USA, 1995. ACM Press.

[24] M. Wardetzky. Convergence of the cotangent formula: An overview. In A. I. Bobenko, J. M. Sullivan, P. Schröder, and G. Ziegler, editors, *Discrete Differential Geometry*, pages 89–112. Birkhäuser, to appear.

[25] G. Xu. Discrete laplace-beltrami operators and their convergence. *Comput. Aided Geom. Des.*, 21(8):767–784, 2004.

[26] G. Xu. Convergence analysis of a discretization scheme for gaussian curvature over triangular surfaces. *Comput. Aided Geom. Des.*, 23(2):193–207, 2006.

[27] K. Zhou, J. Huang, J. Snyder, X. Liu, H. Bao, B. Guo, and H.-Y. Shum. Large mesh deformation using the volumetric graph laplacian. *ACM Trans. Graph.*, 24(3):496–503, 2005.